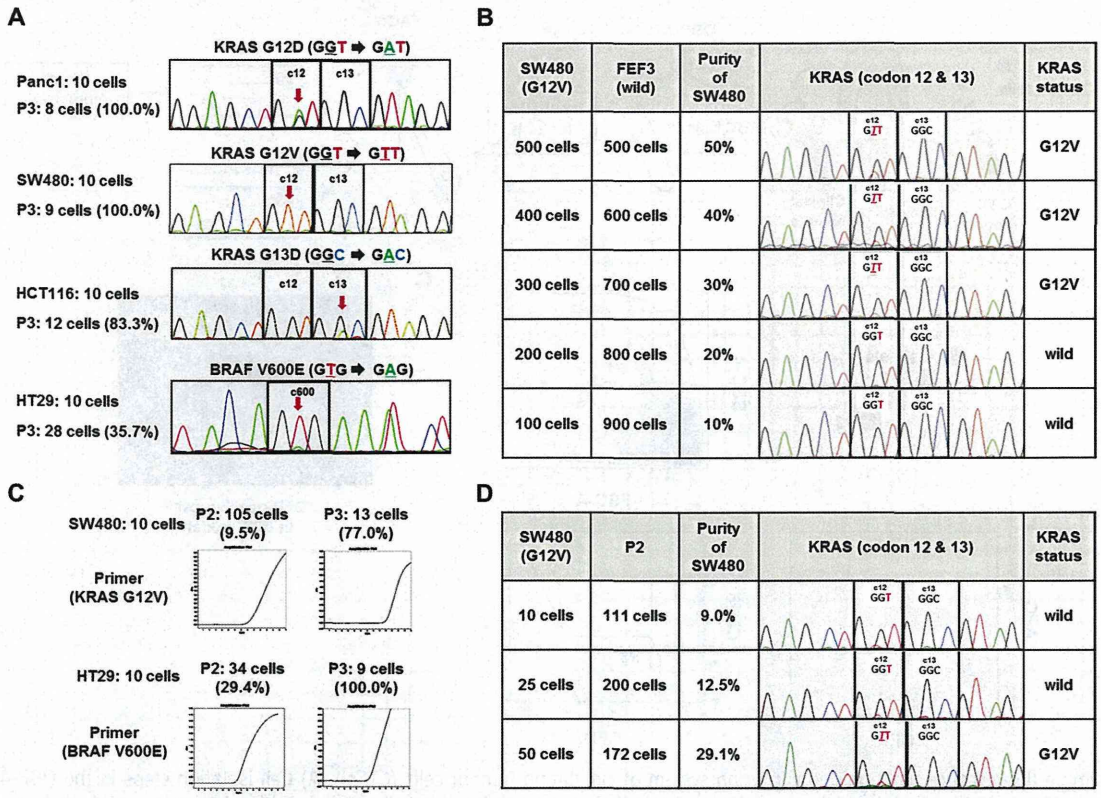

Figure 3 Genetic mutation analysis of human circulating tumour cells (CTCs) by direct sequencing and mutation-specific PCR. (A) Detection of *KRAS* or *BRAF* gene mutation in the CTC models containing 10 human cancer cells by direct sequencing of green fluorescent protein (GFP)-positive cells at the P3 gate. The number of cells in the P3 gate and the mutation pattern in each model are indicated. (B) The minimal purity of tumour cells for direct sequencing to detect the expected gene mutations is evaluated. SW480 (*KRAS* G12 V) cells were mixed with H1299 (*KRAS* wild-type) cells at 50%, 40%, 30%, 20% and 10% of purity ratios. DNA is extracted from cell mixtures, and the *KRAS* gene mutation is analysed by direct sequencing. (C) Allele-specific blocker (ASB)-PCR-mediated detection of *KRAS* and *BRAF* gene mutations in GFP-positive cells at the P2 or P3 gate in the CTC models containing as few as 10 SW480 cells and HT29 cells. When *KRAS* and *BRAF* genes contain targeted mutations, mutation-specific curves cross their threshold of detection. (D) Detection of *KRAS* gene mutation by direct sequencing of GFP-positive cells at the P2 gate without CD45 depletion requires at least 50 SW480 cells in the CTC model.

with mutation-specific primers (see online supplementary figure S3).

When we analysed five human cancer cells mixed with 100 human normal fibroblasts at a purity ratio of approximately 5%, ASB-PCR, using all types of primers, detected the expected mutations in the GFP-positive cells (see online supplementary table 2). In the CTC models containing 10 human cancer cells with different types of *KRAS* and *BRAF* gene mutations, ASB-PCR analysis detected the expected genetic mutations in the GFP-positive cells at the P3 gate (table 1). Moreover, ASB-PCR analysis could detect the genetic alterations in the GFP-positive cells at the P2 gate without exclusion of CD45-positive normal blood cells (figure 3C), whereas at least 50 tumour cells were required for direct sequencing in the

Table 1 Data for mutation-specific PCR for the genetic analysis of CTC models

CTC model				FACS analysis			Genetic analysis			
									Ct values	
Cancer cells	Cell type	Gene status	Number of cancer cells	Gate	Number of GFP-positive cells	Purity of cancer cells (%)	Primer	Amplification	1st PCR	2nd PCR
Panc1	Epithelial	KRAS G12D	10	P2	29	34.5	KRAS G12D	+	37.1	36.1
				P3	6	100.0	KRAS G12D	+	35.3	38.2
SW480	Epithelial	KRAS G12V	10	P2	105	9.5	KRAS G12V	+	45.0	56.5
				P3	13	76.9	KRAS G12V	+	41.6	52.0
HCT116	Epithelial	KRAS G13D	10	P2	23	43.5	KRAS G13D	+	47.5	37.2
				P3	18	55.6	KRAS G13D	+	37.0	44.0
HT29	Epithelial	BRAF V600E	10	P2	34	29.4	BRAF V600E	+	34.0	NA
				P3	9	100.0	BRAF V600E	+	40.0	NA
EMT-induced A549	Mesenchymal	KRAS G12S	10	P2	77	13.0	KRAS G12S	+	41.9	43.5
				P3	17	58.8	KRAS G12S	+	51.1	64.7

CTC, circulating tumour cell; EMT, epithelial–mesenchymal transition; FACS, fluorescence-activated cell sorting; GFP, green fluorescent protein; NA, not amplified.

presence of CD45-positive cells at the P2 gate (figure 3D). These results suggest that the ASB-PCR method is more simple and sensitive than direct sequencing for detection of genetic alterations in heterogeneous populations of CTCs.

Fluorescence-guided capture of EMT-induced and mesenchymal CTCs

Induction of EMT in CTCs has recently been demonstrated in patients with advanced breast cancers.[17] EMT-induced CTCs frequently formed metastatic colonies in the brain and lung of nude mice,[19] suggesting that highly malignant EMT-induced CTCs can be detected to predict metastatic progression in patients with cancer. We used A549 human lung cancer cells with *KRAS* gene mutation (G12S) and EpCAM-negative GIST882 mesenchymal human tumour cells with the *KIT* gene mutation (K642E), which is frequently mutated in more than 70% of GISTs.[30] OBP-401 infection efficiently induced GFP expression in both cell lines in a dose-dependent manner (figure 4A).

When treated with the EMT inducer, TGF-β, A549 cells showed spindle-shape morphological changes (figure 4B) and altered EMT-related biomarker expression, such as EpCAM and E-cadherin downregulation and N-cadherin upregulation (figure 4C). In contrast, CAR expression was not affected after TGF-β treatment (figure 4C). Therefore, OBP-401 efficiently induced GFP expression in the TGF-β-treated A549 cells (figure 4D). In addition, GIST882 cells were confirmed to be EpCAM negative (figure 4E). When 10 EMT-induced A549 cells were spiked in blood samples, the expected genetic mutation (G12S) in the *KRAS* gene was detected by direct sequencing and by ASB-PCR analysis (figure 4F–G and table 1). In contrast, the expected *KIT* gene mutation could be detected at the P3 gate by direct sequencing in the CTC model containing 100 GIST882 cells (figure 4F) but not in that with 10 cells, presumably due to low expression of CAR. These results suggest that the targeted genetic mutations in EMT-induced and mesenchymal CTCs are also detectable by the OBP-401-based CTC capture system, although the sensitivity is dependent on the CAR expression.

Detection of genetic mutations in CTCs in patients with colorectal cancer

Finally, the blood samples obtained from eight patients with *KRAS*- or *BRAF*-mutated colorectal cancers were analysed by the OBP-401-based CTC capture system and by ASB-PCR

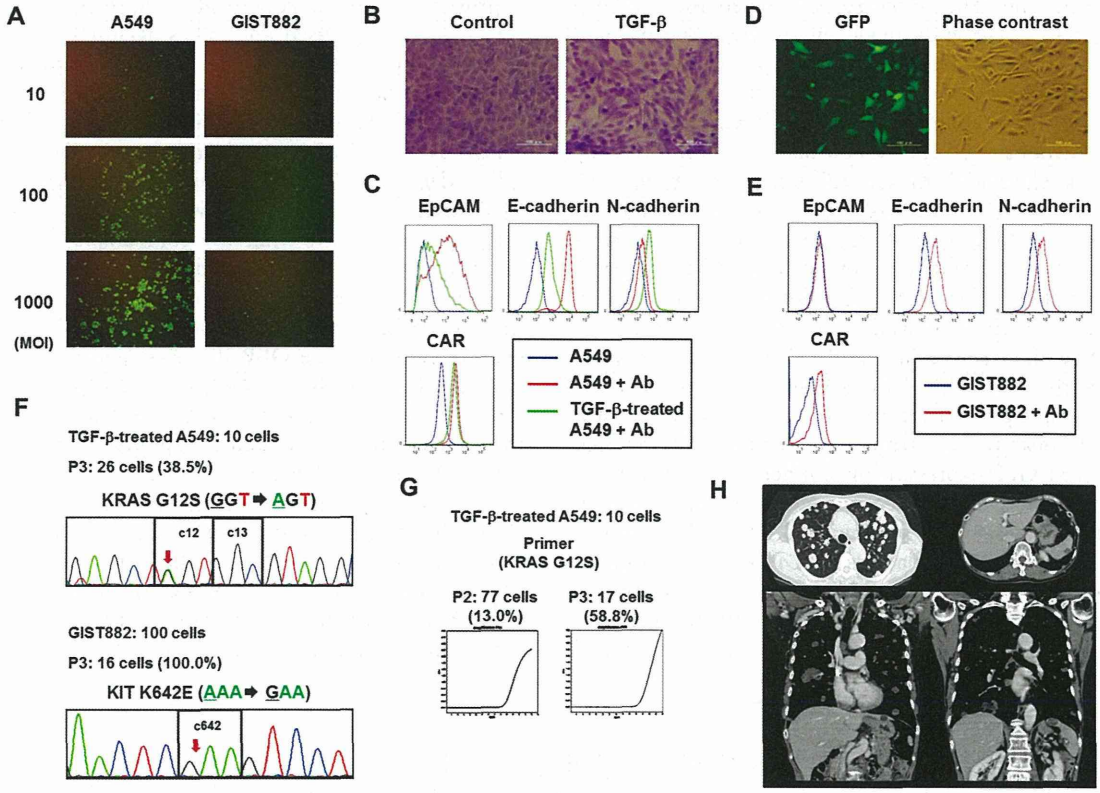

Figure 4 Fluorescence virus-guided capture and genetic mutation analysis of human mesenchymal or epithelial–mesenchymal transition (EMT)-induced tumour cells. (A) A549 human lung cancer cells and GIST882 human gastrointestinal stromal tumour cells are infected with OBP-401 at a multiplicity of infection (MOI) of 10, 100 or 1000 plaque-forming units (PFU) per cell. Green fluorescent protein (GFP) expression is assessed under fluorescence microscope 24 h after virus infection. (B) Morphological change of A549 cells treated with transforming growth factor β (TGF-β). A549 cells are treated with TGF-β (10 ng/mL) for 72 h and stained with crystal violet. Original magnification: ×200. (C) Flow cytometric analysis of epithelial (epithelial cell adhesion molecule (EpCAM) and E-cadherin) and mesenchymal (N-cadherin) cell surface marker and CAR expression in A549 cells treated with or without TGF-β. (D) GFP expression in TGF-β-treated A549 cells after infection with OBP-401 at an MOI of 100 PFU per cell for 24 h. Original magnification: ×200. (E) Flow cytometric analysis of epithelial (EpCAM and E-cadherin) and mesenchymal (N-cadherin) cell-surface markers and coxsackievirus and adenovirus receptor (CAR) expression in GIST882 cells. (F) Detection of *KRAS* and *KIT* gene mutations by direct sequencing of GFP-positive cells at the P3 gate requires 10 TGF-β-treated EMT-induced A549 cells and 100 GIST882 cells in the CTC models, respectively. (G) Detection of *KRAS* gene mutations in GFP-positive cells at the P2 or P3 gate in the CTC models containing as few as 10 of TGF-β-treated A549 cells by allele-specific blocker (ASB)-PCR. Mutation-specific curves for the *KRAS* gene cross their threshold of detection. (H) Representative CT images of patients with colon cancer and lung, spleen and ovary metastases. The primary tumours and CTCs show the *BRAF* V600E mutation.

technology. In preliminary experiments, the number of GFP-positive cells at the P3 gate was less than 10 cells in some clinical blood samples and, therefore, we performed ASB-PCR analysis using GFP-positive cells at the P2 gate. Among the eight blood samples from patients with various stages of colorectal cancer, the same *KRAS* and *BRAF* gene mutations as in the primary tumours were detected in the CTCs of two patients with advanced colorectal cancer (figure 4H and table 2). The other six patients showed no detectable genetic abnormalities in blood samples, although *KRAS* gene mutations were observed in their primary tumours. Three patients without metastatic lesions did not have a large CTC count, and chemotherapeutic treatment in the other three patients with metastatic disease may have resulted in a reduced number of CTCs. Although further large-scale clinical trials are required, our results suggest that the OBP-401-based telomerase-dependent biological CTC capture system is useful for genetic analysis of CTCs in blood samples from patients with cancer.

DISCUSSION

The co-development of a targeted therapy together with its companion diagnostic test, which guides selection of patients and provides surrogate markers to monitor responses, is a key part of personalised medicine. The selection of targeted therapies for individual patients is currently made by analysing the primary tumours, although there are very few cells within the primary tumours that are responsible for metastasis or recurrence, and these cells may have additional genetic abnormalities. The present study demonstrated that CTCs obtained non-invasively are a promising alternative to surgically resected or biopsied tumour tissues for real-time molecular characterisation. A telomerase-dependent biological CTC capture system was clinically useful for the detection of mutations in different target genes, such as *KRAS*, *BRAF* and *KIT*, even in EpCAM-negative cells among highly heterogeneous CTC populations.

We applied telomerase-specific OBP-401 to selectively label human neoplastic cells with GFP signals and confirmed its broad infectivity independent of EpCAM expression, which was consistent with observations from our previous reports that OBP-401 induced GFP expression in epithelial and mesenchymal types of tumour cells.[24 25] Recent studies demonstrated that highly metastatic tumour cells are involved in EpCAM-positive and EpCAM-negative subpopulations of CTCs in the blood of patients with breast cancer.[18 19] During anticancer treatment, the characteristics of CTCs dynamically alternate between epithelial and mesenchymal types of CTCs within individual patients with cancer.[17] Further, platelet-derived TGF-β secretion induces EMT with metastatic potential in CTCs.[31] These findings indicate that single CTCs frequently turn the EMT switch on or off in the microenvironment of the bloodstream. In contrast, high telomerase activity is a general functional biomarker for stabilisation of the telomere in epithelial and mesenchymal malignant tumour cells during aberrant proliferation. In fact, high *hTERT* mRNA levels have been detected in the blood samples of patients with cancer.[32–34] Moreover, hTERT overexpression has been shown to be positively associated with EMT induction in human cancer cells.[35] When the telomerase activity in the CTCs is suppressed in circulating cells, these CTCs undergo programmed cell death (ie, apoptosis or senescence). Thus, the telomerase activity may be superior to unstable epithelial cell marker as a general biomarker for the detection of viable CTCs in the blood. Moreover, GFP-labelled CTCs by OBP-401 infection are considered to be useful for direct determination of drug sensitivity and metastatic potential, and determination of tumour heterogeneity.[36–39]

A number of approaches based on the physical and biological properties of CTCs have been studied to distinguish CTCs from surrounding normal haematopoietic cells and to capture them for further analysis. The CellSearch system, which is the only test approved by the US Food and Drug Administration to detect CTCs, uses magnetised antibodies against EpCAM for positive selection and uses CD45 for leukocyte depletion. Another popular technology for CTC enrichment is a microfluidic-based device called the CTC-chip; this device can isolate and analyse CTCs using EpCAM-coated microposts. Our OBP-401-based CTC detection has been previously compared with the CellSearch assay in patients with metastatic breast cancer.[40] Although both assays exhibited comparable detection rates, the number of CTC-positive cells between both assays was not significantly correlated. Nine out of 50 (18%) cases were positive by both methods, while 12 (24%) and 18 (36%) patients showed positive cells with the OBP-401 assay and the CellSearch assays individually, respectively. We speculate that CTCs detected by OBP-401 primarily detect EpCAM-negative tumour cells while the CellSearch method detects epithelial non-tumour cells as well, including circulating fibroblasts.

Our strategy involves conventional FACS to capture OBP-401-labelled GFP-positive CTCs. OBP-401 infection increases the signal-to-background ratio as a tumour-specific probe, because the fluorescent signal can be amplified only in viable human tumour cells by viral replication. We excluded the autofluorescence-positive cells at the P2 gate and the

Table 2 Data for mutation-specific PCR for the genetic analysis of patient samples

Patients				FACS analysis		Genetic analysis			
								Ct values	
Tumour site	Stage	Gene status of primary tumour	Metastasis	Gate	Number of GFP-positive cells	Primer	Amplification	1st PCR	2nd PCR
Colon	I	KRAS G13D	None	P2	6	KRAS G13D	–	NA	NA
Colon	II	KRAS G13D	None	P2	20	KRAS G13D	–	NA	NA
Colon	II	KRAS G12D	Liver	P2	95	KRAS G12D	+	55.1	61.0
Colon	III	KRAS G13D	None	P2	913	KRAS G13D	–	NA	NA
Colon	III	BRAF V600E	Lung, spleen, ovary	P2	138	BRAF V600E	+	63.0	NA
Colon	IV	KRAS G12D	Liver	P2	14	KRAS G12D	–	NA	NA
Colon	IV	KRAS G12V	Liver	P2	74	KRAS G12V	–	NA	NA
Colon	IV	KRAS G12V	Lung	P2	53	KRAS G12V	–	NA	NA

CTC, circulating tumour cell; FACS, fluorescence-activated cell sorting; GFP, green fluorescent protein; NA, not amplified.

haematopoietic CD45-positive cells at the P3 gate. When at least 10 human cancer cells were spiked in 5 mL of blood from a healthy volunteer, the number of GFP-positive cells detected at the P3 gate was almost the same as the number of spiked tumour cells, suggesting that the P3 gate contains pure CTCs. However, the P2 gate may be contaminated with non-CTC cells. Indeed, ASB-PCR analysis detected the expected gene mutations in the *KRAS* and *BRAF* genes at the P2 gate, whereas the P3 gate was necessary when direct sequencing was applied. Recently, a combination of the CellSearch system and genetic analysis was also performed to detect genetic mutations in rare CTCs from patients with cancer. Mostert *et al*[41] compared the three types of PCR-based genetic analysis of CTCs, and ASB-PCR, used in our study, was the most sensitive method for detecting *KRAS* and *BRAF* gene mutations in the CTCs from patients with metastatic colorectal cancers. In addition, as our data demonstrated that direct sequencing was limited if CTC-derived DNA had more than 30% purity, we conclude that, together with FACS-isolated OBP-401-infected GFP-expressing CTCs, ASB-PCR is a suitable assay for non-invasive companion diagnostics in patients with cancer. The specificity of the ASB-PCR assay allowed us to use the P2 gate for clinical samples even in the presence of non-CTC cells.

Mutation in *KRAS* and *BRAF* genes is highly associated with resistance to the anti-EGFR antibody, cetuximab, in patients with colorectal cancer.[42 43] In fact, the appearance of *KRAS* gene mutant DNA is associated with resistance to cetuximab in patients with KRAS wild-type colorectal cancers.[44] In patients with colorectal cancer, the frequency of the *KRAS* and *BRAF* gene mutations is significantly higher in liver metastasis than in primary tumours,[45] and *KRAS* and *BRAF* gene mutant status is significantly associated with poor outcomes.[46] These findings suggest that genetic analysis for the *KRAS* and *BRAF* gene mutation in CTCs can be used as a 'liquid biopsy' to monitor resistance to cetuximab and to predict metastatic potential in patients with KRAS wild-type colorectal cancers.

It is also worth noting that the OBP-401-based biological CTC capture system is applicable to the genetic analysis of CTCs with mesenchymal characteristics, including GISTs and osteosarcomas,[25] although the CellSearch system is also useful for detection of epithelial CTCs. Approximately 80% of GIST cells harbour a mutation in the *KIT* gene,[30] which is significantly associated with disease recurrence and poor outcomes.[47] Recently, the small-molecule tyrosine-kinase inhibitor imatinib has been shown to be effective against KIT-mutated GIST that is refractory to conventional chemotherapy.[48] In contrast, bone and soft tissue sarcoma cells, which make up one of the most notorious types of malignant mesenchymal tumours, are also detectable as GFP-positive cells by OBP-401 infection.[25] Frequent lung metastasis has been shown to be a poor prognostic factor in patients with osteosarcoma, but the potential of CTC enumeration in patients with osteosarcoma remains to be elucidated. Thus, the characterisation of CTCs, using the OBP-401-based biological CTC capture system, may be a useful strategy for monitoring metastatic progression in patients with GIST or osteosarcomas, as well as those with epithelial malignant tumours.

The combination of the OBP-401-based CTC capture system and genetic analysis using ASB-PCR detected *KRAS* and *BRAF* mutations in blood samples obtained from patients with colorectal cancer, and these mutations were identical to those seen in the primary tumours. This novel 'liquid biopsy' via a simple blood test could be carried out in real time and enables optimised and timely decisions for therapeutic intervention. However, the technology has to be further validated in large clinical studies with defined endpoints. In addition, one limitation of our study was that it was difficult for ASB-PCR to detect uncommon genetic abnormalities. Regardless, when frequently occurring genetic mutations are targeted for the surveillance of CTCs, the ASB-PCR method would be a useful and highly sensitive method for detecting small numbers of CTCs with genetic mutations. In contrast, if the identification of genetic traits in highly metastatic CTCs is the main goal, a genome-wide approach should be considered for the genetic analysis of CTCs. For example, genome-wide transcriptome analysis has been performed to identify a wide range of copy number alterations in entire CTC populations, using array-comprehensive genomic hybridisation (aCGH).[49] Moreover, genetic analysis in a single CTC has been recently used to clarify global gene alterations using aCGH and next-generation sequencing.[50 51] Thus, the comprehensive analysis of genetic alterations in individual CTCs from patients with cancer would provide novel insight into the identification of genetic signatures associated with metastatic progression.

In summary, we established a telomerase-dependent biological CTC capture system for genotyping of epithelial, mesenchymal, and EMT-induced types of CTCs using OBP-401 and FACS analysis. This technology facilitates the surveillance of genetic alterations in viable CTCs in patients with cancer. Large-scale clinical studies of this strategy are warranted.

Acknowledgements We thank Yukinari Isomoto and Tomoko Sueishi for their technical support.

Contributors Conception and design: HT, SK, TF; development of methodology: KS, HT, YH, TN; acquisition of data: KS, YH, YM; analysis and interpretation of data: KS, HT, HK, SK, TF; writing, review and/or revision of the manuscript: KS, HT, AG, TF; administrative, technical, or material support: MN, SK, YU; study supervision: TF.

Funding This study was supported by grants-in-aid from the Ministry of Education Culture, Sports, Science and Technology, Japan (T. Fujiwara, H. Tazawa, S. Kagawa) and grants from the Ministry of Health, Labour and Welfare, Japan (T. Fujiwara).

Competing interests Yasuo Urata is the president and CEO of Oncolys BioPharma, Inc., the manufacturer of OBP-401 (TelomeScan). Hiroshi Tazawa and Toshiyoshi Fujiwara are consultants for Oncolys BioPharma, Inc. The other authors have no real or potential conflicts of interest to declare.

Ethics approval Okayama University.

Provenance and peer review Not commissioned; externally peer reviewed.

REFERENCES

1 Ong FS, Das K, Wang J, *et al*. Personalized medicine and pharmacogenetic biomarkers: progress in molecular oncology testing. *Expert Rev Mol Diagn* 2012;12:593–602.
2 Hurvitz SA, Hu Y, O'Brien N, *et al*. Current approaches and future directions in the treatment of HER2-positive breast cancer. *Cancer Treat Rev* 2013;39:219–29.
3 Pietrantonio F, De Braud F, Da Prat V, *et al*. A review on biomarkers for prediction of treatment outcome in gastric cancer. *Anticancer Res* 2013;33:1257–66.
4 Anderson SM. Laboratory methods for KRAS mutation analysis. *Expert Rev Mol Diagn* 2011;11:635–42.
5 Kwak EL, Bang YJ, Camidge DR, *et al*. Anaplastic lymphoma kinase inhibition in non-small-cell lung cancer. *N Engl J Med* 2010;363:1693–703.
6 Maemondo M, Inoue A, Kobayashi K, *et al*. Gefitinib or chemotherapy for non-small-cell lung cancer with mutated EGFR. *N Engl J Med* 2010;362:2380–8.
7 Cross NC, White HE, Muller MC, *et al*. Standardized definitions of molecular response in chronic myeloid leukemia. *Leukemia* 2012;26:2172–5.
8 Zieba A, Grannas K, Soderberg O, *et al*. Molecular tools for companion diagnostics. *N Biotechnol* 2012;29:634–40.
9 Fridlyand J, Simon RM, Walrath JC, *et al*. Considerations for the successful co-development of targeted cancer therapies and companion diagnostics. *Nat Rev Drug Discov* 2013;12:743–55.
10 Ashworth T. A case of cancer in which cells similar to those in the tumours were seen in blood after death. *Aust Med J* 1869;14:146–9.
11 Cristofanilli M, Budd GT, Ellis MJ, *et al*. Circulating tumor cells, disease progression, and survival in metastatic breast cancer. *N Engl J Med* 2004;351:781–91.
12 Miller MC, Doyle GV, Terstappen LW. Significance of circulating tumor cells detected by the CellSearch system in patients with metastatic breast colorectal and prostate cancer. *J Oncol* 2010;2010:617421.

13 Maheswaran S, Sequist LV, Nagrath S, *et al*. Detection of mutations in EGFR in circulating lung-cancer cells. *N Engl J Med* 2008;359:366–77.
14 Chaffer CL, Weinberg RA. A perspective on cancer cell metastasis. *Science* 2011;331:1559–64.
15 Joosse SA, Pantel K. Biologic challenges in the detection of circulating tumor cells. *Cancer Res* 2013;73:8–11.
16 Konigsberg R, Obermayr E, Bises G, *et al*. Detection of EpCAM positive and negative circulating tumor cells in metastatic breast cancer patients. *Acta Oncol* 2011;50:700–10.
17 Yu M, Bardia A, Wittner BS, *et al*. Circulating breast tumor cells exhibit dynamic changes in epithelial and mesenchymal composition. *Science* 2013;339:580–4.
18 Baccelli I, Schneeweiss A, Riethdorf S, *et al*. Identification of a population of blood circulating tumor cells from breast cancer patients that initiates metastasis in a xenograft assay. *Nat Biotechnol* 2013;31:539–44.
19 Zhang L, Ridgway LD, Wetzel MD, *et al*. The identification and characterization of breast cancer CTCs competent for brain metastasis. *Sci Transl Med* 2013;5:180ra48.
20 Pecot CV, Bischoff FZ, Mayer JA, *et al*. A novel platform for detection of CK+ and CK– CTCs. *Cancer Discov* 2011;1:580–6.
21 Yokobori T, Iinuma H, Shimamura T, *et al*. Plastin3 is a novel marker for circulating tumor cells undergoing the epithelial–mesenchymal transition and is associated with colorectal cancer prognosis. *Cancer Res* 2013;73:2059–69.
22 Hiyama E, Hiyama K. Telomerase as tumor marker. *Cancer Lett* 2003;194:221–33.
23 Kyo S, Inoue M. Complex regulatory mechanisms of telomerase activity in normal and cancer cells: how can we apply them for cancer therapy? *Oncogene* 2002;21:688–97.
24 Kishimoto H, Kojima T, Watanabe Y, *et al*. In vivo imaging of lymph node metastasis with telomerase-specific replication-selective adenovirus. *Nat Med* 2006;12:1213–19.
25 Sasaki T, Tazawa H, Hasei J, *et al*. A simple detection system for adenovirus receptor expression using a telomerase-specific replication-competent adenovirus. *Gene Therapy* 2013;20:112–18.
26 Kojima T, Hashimoto Y, Watanabe Y, *et al*. A simple biological imaging system for detecting viable human circulating tumor cells. *J Clin Invest* 2009;119:3172–81.
27 Ito H, Inoue H, Sando N, *et al*. Prognostic impact of detecting viable circulating tumour cells in gastric cancer patients using a telomerase-specific viral agent: a prospective study. *BMC Cancer* 2012;12:346.
28 Takakura M, Kyo S, Nakamura M, *et al*. Circulating tumour cells detected by a novel adenovirus-mediated system may be a potent therapeutic marker in gynaecological cancers. *Br J Cancer* 2012;107:448–54.
29 Morlan J, Baker J, Sinicropi D. Mutation detection by real-time PCR: a simple, robust and highly selective method. *PLoS One* 2009;4:e4584.
30 Heinrich MC, Blanke CD, Druker BJ, *et al*. Inhibition of KIT tyrosine kinase activity: a novel molecular approach to the treatment of KIT-positive malignancies. *J Clin Oncol* 2002;20:1692–703.
31 Labelle M, Begum S, Hynes RO. Direct signaling between platelets and cancer cells induces an epithelial-mesenchymal-like transition and promotes metastasis. *Cancer Cell* 2011;20:576–90.
32 Wang JY, Lin SR, Wu DC, *et al*. Multiple molecular markers as predictors of colorectal cancer in patients with normal perioperative serum carcinoembryonic antigen levels. *Clin Cancer Res* 2007;13:2406–13.
33 Uen YH, Lin SR, Wu DC, *et al*. Prognostic significance of multiple molecular markers for patients with stage II colorectal cancer undergoing curative resection. *Ann Surg* 2007;246:1040–6.
34 Bertorelle R, Briarava M, Rampazzo E, *et al*. Telomerase is an independent prognostic marker of overall survival in patients with colorectal cancer. *Br J Cancer* 2013;108:278–84.
35 Liu Z, Li Q, Li K, *et al*. Telomerase reverse transcriptase promotes epithelial–mesenchymal transition and stem cell-like traits in cancer cells. *Oncogene* 2013;32:4203–13.
36 Mitsiades CS, Mitsiades NS, Bronson RT, *et al*. Fluorescence imaging of multiple myeloma cells in a clinically relevant SCID/NOD in vivo model: biologic and clinical implications. *Cancer Res* 2003;63:6689–96.
37 Kolostova K, Pinterova D, Hoffman RM, *et al*. Circulating human prostate cancer cells from an orthotopic mouse model rapidly captured by immunomagnetic beads and imaged by GFP expression. *Anticancer Res* 2011;31:1535–9.
38 Menen RS, Pinney E, Kolostova K, *et al*. A rapid imageable in vivo metastasis assay for circulating tumor cells. *Anticancer Res* 2011;31:3125–8.
39 Menen R, Zhao M, Zhang L, *et al*. Comparative chemosensitivity of circulating human prostate cancer cells and primary cancer cells. *Anticancer Res* 2012;32:2881–4.
40 Kim SJ, Masago A, Tamaki Y, *et al*. A novel approach using telomerase-specific replication-selective adenovirus for detection of circulating tumor cells in breast cancer patients. *Breast Cancer Res Treat* 2011;128:765–73.
41 Mostert B, Jiang Y, Sieuwerts AM, *et al*. KRAS and BRAF mutation status in circulating colorectal tumor cells and their correlation with primary and metastatic tumor tissue. *Int J Cancer* 2013;133:130–41.
42 Lievre A, Bachet JB, Le Corre D, *et al*. KRAS mutation status is predictive of response to cetuximab therapy in colorectal cancer. *Cancer Res* 2006;66:3992–5.
43 Laurent-Puig P, Cayre A, Manceau G, *et al*. Analysis of PTEN, BRAF, and EGFR status in determining benefit from cetuximab therapy in wild-type KRAS metastatic colon cancer. *J Clin Oncol* 2009;27:5924–30.
44 Misale S, Yaeger R, Hobor S, *et al*. Emergence of KRAS mutations and acquired resistance to anti-EGFR therapy in colorectal cancer. *Nature* 2012;486:532–6.
45 Oliveira C, Velho S, Moutinho C, *et al*. KRAS and BRAF oncogenic mutations in MSS colorectal carcinoma progression. *Oncogene* 2007;26:158–63.
46 Umeda Y, Nagasaka T, Mori Y, *et al*. Poor prognosis of KRAS or BRAF mutant colorectal liver metastasis without microsatellite instability. *J Hepatobiliary Pancreat Sci* 2013;20:223–33.
47 Taniguchi M, Nishida T, Hirota S, *et al*. Effect of c-kit mutation on prognosis of gastrointestinal stromal tumors. *Cancer Res* 1999;59:4297–300.
48 Tuveson DA, Willis NA, Jacks T, *et al*. STI571 inactivation of the gastrointestinal stromal tumor c-KIT oncoprotein: biological and clinical implications. *Oncogene* 2001;20:5054–8.
49 Magbanua MJ, Sosa EV, Roy R, *et al*. Genomic profiling of isolated circulating tumor cells from metastatic breast cancer patients. *Cancer Res* 2013;73:30–40.
50 Ramskold D, Luo S, Wang YC, *et al*. Full-length mRNA-Seq from single-cell levels of RNA and individual circulating tumor cells. *Nat Biotechnol* 2012;30:777–82.
51 Heitzer E, Auer M, Gasch C, *et al*. Complex tumor genomes inferred from single circulating tumor cells by array-CGH and next-generation sequencing. *Cancer Res* 2013;73:2965–75.

Biological Ablation of Sentinel Lymph Node Metastasis in Submucosally Invaded Early Gastrointestinal Cancer

Satoru Kikuchi[1], Hiroyuki Kishimoto[1], Hiroshi Tazawa[1,2], Yuuri Hashimoto[1], Shinji Kuroda[1], Masahiko Nishizaki[1], Takeshi Nagasaka[1], Yasuhiro Shirakawa[1], Shunsuke Kagawa[1], Yasuo Urata[3], Robert M Hoffman[4,5] and Toshiyoshi Fujiwara[1]

[1]Department of Gastroenterological Surgery, Okayama University Graduate School of Medicine, Dentistry and Pharmaceutical Sciences, Okayama, Japan; [2]Center for Innovative Clinical Medicine, Okayama University Hospital, Okayama, Japan; [3]Oncolys BioPharma, Inc., Tokyo, Japan; [4]Department of Surgery, University of California, San Diego, California, USA; [5]AntiCancer, Inc., San Diego, California, USA

Currently, early gastrointestinal cancers are treated endoscopically, as long as there are no lymph node metastases. However, once a gastrointestinal cancer invades the submucosal layer, the lymph node metastatic rate rises to higher than 10%. Therefore, surgery is still the gold standard to remove regional lymph nodes containing possible metastases. Here, to avoid prophylactic surgery, we propose a less-invasive biological ablation of lymph node metastasis in submucosally invaded gastrointestinal cancer patients. We have established an orthotopic early rectal cancer xenograft model with spontaneous lymph node metastasis by implantation of green fluorescent protein (GFP)-labeled human colon cancer cells into the submucosal layer of the murine rectum. A solution containing telomerase-specific oncolytic adenovirus was injected into the peritumoral submucosal space, followed by excision of the primary rectal tumors mimicking the endoscopic submucosal dissection (ESD) technique. Seven days after treatment, GFP signals had completely disappeared indicating that sentinel lymph node metastasis was selectively eradicated. Moreover, biologically treated mice were confirmed to be relapse-free even 4 weeks after treatment. These results indicate that virus-mediated biological ablation selectively targets lymph node metastasis and provides a potential alternative to surgery for submucosal invasive gastrointestinal cancer patients.

Received 21 October 2014; accepted 14 December 2014; advance online publication 20 January 2015. doi:10.1038/mt.2014.244

INTRODUCTION

Due to recent advances in endoscopic technology, early gastrointestinal cancers, which are defined as those that invade no more deeply than the submucosa, are treated endoscopically.[1–3] Endoscopic submucosal dissection (ESD) or local tumor excisions that allow en bloc resection, which lead to more precise histological evaluation and more potential for cure, are considered clinically relevant for early gastrointestinal cancer. A complete local resection of *in situ* or intramucosal tumor is acceptable as a curative treatment due to little risk of lymph node metastasis.[4–7] However, lymph node metastasis is typically found in submucosal invasive gastrointestinal cancer such as esophageal, gastric and colorectal cancer, at an approximate frequency of greater than 10%.[8–11] Since it is difficult to determine submucosally invaded lesions with the risk of lymph node metastasis without pathological evaluation, these patients are treated surgically to remove possibly metastasized lymph nodes, even though primary early gastrointestinal cancer itself is technically resectable with ESD. This means that most submucosal invasive gastrointestinal cancer patients, who are node-negative, routinely undergo unnecessary surgery. Thus, a less invasive way to selectively treat lymph node metastasis would benefit these patients by allowing them to avoid a prophylactic surgery.

Sentinel lymph node metastasis represents the initial spread of malignant tumors from the primary site. Metastatic lymph nodes as well as migrating tumor cells in the draining lymph vessels have to be treated to prevent recurrence and, therefore, anticancer agents that spread over the regional lymphatic area are required. For sentinel lymph node mapping, submucosal injection of a visible dye such as methylene blue or indocyanine green (ICG) allows an adequate regional diffusion in the lymphatic area.[12] It has also been reported that human adenovirus can be effectively transported into the lymphatic circulation in murine models.[13,14] Oncolytic viruses that selectively replicate in tumor cells and lyse infected cells have been developed as anticancer agents.[15–18] These viruses are designed to induce virus-mediated lysis of infected cells after selective viral replication within the tumor cells.

In this study, we evaluated whether a telomerase-dependent, tumor-killing replicating adenoviral agent (OBP-301) that was administered submucosally prior to the primary tumor resection could purge lymph node metastasis in an orthotopic early rectal cancer xenograft model with spontaneous lymph node metastasis. The steps of this procedure mimic the procedures of ESD

Correspondence: Toshiyoshi Fujiwara, Department of Gastroenterological Surgery, Okayama University Graduate School of Medicine, Dentistry, and Pharmaceutical Sciences, 2-5-1 Shikata-cho, Kita-ku, Okayama 700–8558, Japan. E-mail: toshi_f@md.okayama-u.ac.jp

for gastrointestinal cancer in the clinical setting. The successful elimination of sentinel lymph node metastasis indicates that concurrent submucosal injection of OBP-301 and endoscopic tumor removal might be a paradigm-changing therapeutic alternative to prophylactic surgery for patients with submucosally invaded gastrointestinal cancer.

RESULTS

In vitro cytopathic effect of the virus on human colorectal cancer cells

OBP-301 (Telomelysin) is an attenuated adenovirus that drives the *E1A* and *E1B* genes under the human telomerase reverse transcriptase (hTERT) promoter and is capable of killing human epithelial as well as mesenchymal malignant cells in a telomerase-dependent manner (**Supplementary Figure S1a**).[19–21] To assess the cytopathic effect (CPE) of OBP-301 on human colorectal cancer cells, green fluorescent protein (GFP)-labeled HCT-116 or Colo 205 cells were infected either with OBP-301 or with a replication-deficient, E1-deleted adenovirus, dl312 and were photographed using a fluorescent microscope after viral infection. Both HCT-116-GFP and Colo 205-GFP cells infected with OBP-301 at an MOI of 10 exhibited rapid cell death by 72 hours after virus infection, whereas cells treated with the same MOI of dl312 or with PBS showed no morphological change (**Figure 1a** and **Supplementary Figure S2**). The XTT cell-viability assay also demonstrated that OBP-301 infection induced cell death in a dose-dependent fashion both in HCT-116-GFP and Colo 205-GFP cells, whereas infection with dl312 did not show significant CPE at multiplicity of infections (MOIs) of up to 100 (**Figure 1b**). We previously reported that no apparent CPE was observed in normal human cell lines after OBP-301 infection.[19]

Sentinel lymph node metastasis in an orthotopic rectal cancer xenograft model

A submucosally invaded early rectal tumor model was established by inoculating HCT-116-GFP or Colo205-GFP human colorectal cancer cells orthotopically into athymic *nu/nu* mice. Seven days after implantation of GFP-labeled cancer cells into the submucosal layer of the rectum, the mice developed minute rectal tumors that were clearly visible by fluorescence imaging of GFP signals (**Figure 2a**, **Supplementary Figures S3 and S5a**). Histopathological examination of the excised primary rectal tumors showed submucosal tumor formation composed of implanted cancer cells with no muscularis propria invasion. Examination under high magnification showed cancer cell-filled lymphatic vessels in the submucosal layer (**Figure 2b**). The metastatic status of regional lymph nodes was easily assessed at laparotomy, by detection of cancer cell-derived GFP signals in the lymph node (**Figure 2c,d**). A series of experiments confirmed that the percent metastasis to the sentinel lymph node on day 7 after tumor cell inoculation in mice implanted with HCT-116-GFP or Colo 205-GFP was 78.5% (33/42) and 62.5% (25/40), respectively.

Viral trafficking to lymph nodes and selective replication in metastatic foci

The lymphatic system is a major pathway for the metastatic spread of cancers as well as for the regional distribution of

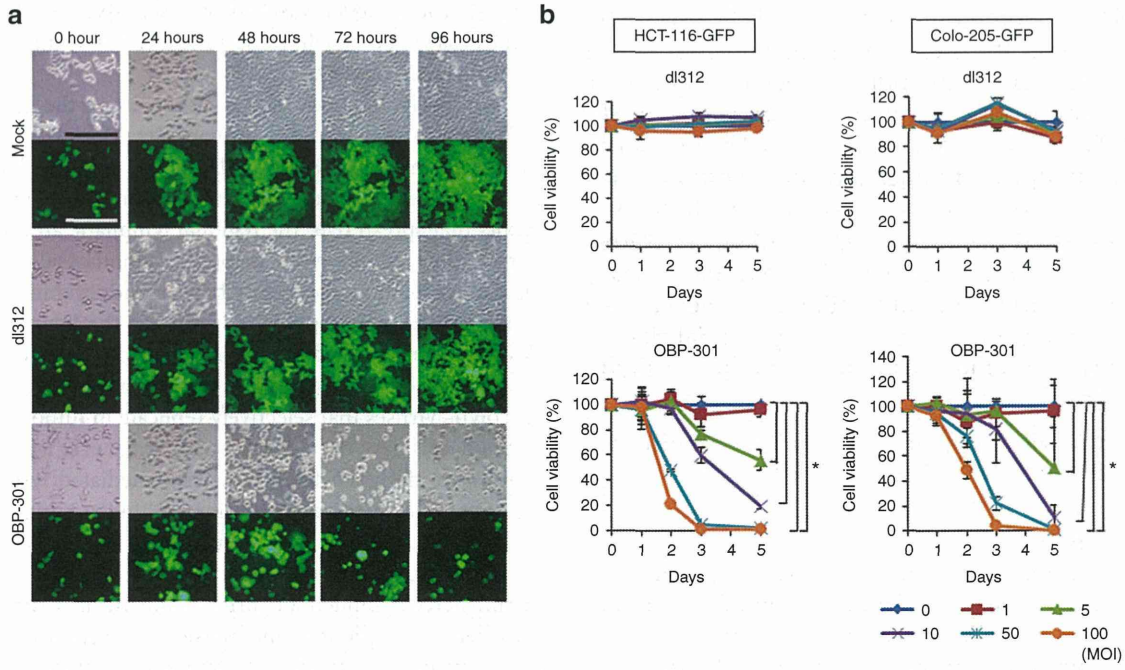

Figure 1 Cytopathic effect of OBP-301 on human colorectal cancer cell lines. (**a**) HCT-116-GFP cells were infected with replication-deficient adenovirus dl312 or OBP-301 at a multiplicity of injection (MOI) of 10. Cell morphology and GFP expression were evaluated at the indicated time points by phase-contrast (top panels) and fluorescence (bottom panels) microscopy, respectively. Magnification: ×200. Scale bar, 200 μm. (**b**) HCT-116-GFP and Colo 205-GFP cells were infected with OBP-301 or dl312 at the indicated MOIs and cell survival was quantified over 5 days using the XTT assay. The cell viability of a mock-treated group on each day was considered 100% and the percent cell viability was calculated. Data are means ± SD. Statistical significance was defined as $^*P < 0.05$.

biological mediators including fluids, proteins, chemicals, cells and drugs. Prior to injection of virus, we first assayed the ability of an injected solution to reach the draining lymph nodes. For this purpose, we investigated the diffusion pattern of a 1% indigo-carmine-blue dye solution that was peritumorally injected into the submucosal space of the rectum in the orthotopic rectal cancer mouse models. Intense blue staining was detected in regional lymph nodes as early as 1 minute after injection of the dye, indicating that an injected solution could rapidly enter the lymphatics and spread to the draining lymph nodes (**Supplementary Figure S4**).

To verify that virus could move to regional lymph nodes and further infect tumor cells in these nodes after peritumoral injection into the submucosal space of the mouse rectum, we used RFP-labeled HCT-116 cells and GFP-expressing OBP-401 (TelomeScan). OBP-401 was constructed by inserting the *GFP* gene under the control of the cytomegalovirus promoter at the deleted E3 region of OBP-301 (ref. [13,22]) (**Supplementary Figure S1**). When RFP-expressing sentinel lymph node metastases were established, mice were peritumorally injected with OBP-401 into the rectal submucosal space. Six days after OBP-401 injection, virus-induced GFP expression was detected in the sentinel lymph nodes by fluorescence imaging. The merged images showed that the viral GFP signals were coincident with RFP fluorescence of metastatic foci in sentinel lymph nodes (**Figure 3a,b**). Moreover, immunohistochemical staining for adenoviral E1A protein demonstrated that the E1A protein was selectively expressed in the metastatic area in lymph nodes, confirming the presence of replicating OBP-301 in metastatic tumor cells (**Figure 3c**). These results indicate that, after injection into the submucosal space, OBP-301 can traffic through the lymphatics to the regional lymph nodes and selectively replicate in cancer cells in metastatic lymph nodes.

Virus-mediated biological ablation of metastatic foci in regional lymph nodes

We next examined whether peritumoral submucosal injection of OBP-301 followed by primary tumor resection could ablate lymph node metastasis in the orthotopic submucosally invaded rectal cancer mouse models. Seven days after inoculation with HCT-116-GFP human colorectal cancer cells, mice that had successfully established GFP-expressing lymph node metastasis were selected by fluorescence imaging at laparotomy, and were further studied (**Figure 4a**). When primary rectal tumors were surgically removed, a solution containing OBP-301 (1×10^9 plaque forming units (PFU)/30 µl PBS) was peritumorally injected into the submucosal space as a fluid cushion. This fluid cushion was used to lift up the tumors in order to precisely preserve the rectal muscular layer (**Supplementary Figure S5**). These procedures mimicked the standard ESD technique in humans. Seven days after tumor resection, a second-look laparotomy was performed to assess tumor progression in the lymph nodes. Mice treated with PBS (30 µl), cisplatin (30 µl of concentrated original solution; 30 µg), or dl312 (1×10^9 PFU/30 µl PBS) showed more intense GFP expression, and GFP expression over a wider area in metastatic lymph nodes, whereas GFP signals were undetectable in mice that had received OBP-301, indicating the complete eradication of metastatic tumor cells in these mice (**Figure 4b**).

To more precisely quantify virus-mediated effects on lymph node metastasis, fluorescence intensities were measured using image analysis software. Preinjection of OBP-301 prior to primary tumor resection significantly reduced GFP signals compared to the other groups in both the HCT-116 and Colo 205 mouse models (**Figure 5a**). Quantification of the amounts of human cancer cells in mouse lymph nodes by using a highly sensitive real-time PCR method that targets human *Alu* sequences also demonstrated that OBP-301 completely eradicated metastatic human cancer cells (**Figure 5b**). Furthermore, lower viral doses (1×10^7 or 1×10^6

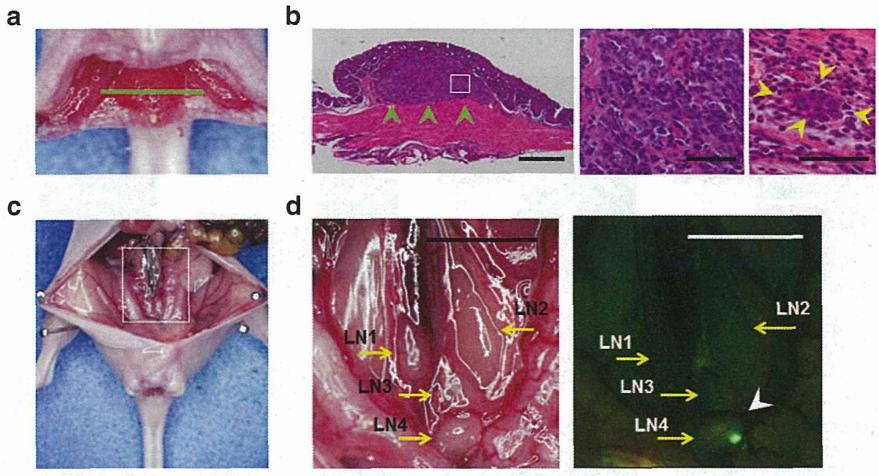

Figure 2 Submucosally invaded orthotopic xenografts of human colorectal cancer cells and subsequent development of sentinel lymph node metastasis. HCT-116-GFP human colorectal cancer cells (1.5×10^6 cells/mouse) were submucosally inoculated into the rectum of nude mice. (**a**) Macroscopic appearance of an HCT-116-GFP rectal tumor at 7 days after tumor inoculation. Green line, direction of tumor cross-sections. (**b**) Histological sections stained with hematoxylin and eosin showing local growth of the HCT-116-GFP tumor in the submucosal layer of the rectum (green arrowheads). Scale bar, 500 µm. Left, ×40 magnification; middle, detail of the boxed region of the left panel, ×400; right, lymphatic vessel invasion of HCT-116-GFP cancer cells (yellow arrowheads), ×400 magnification. (**c**) Gross appearance of the abdominal cavity in a representative mouse. Seven days after inoculation of HCT-116-GFP cancer cells, mice were assessed for lymph node metastasis at laparotomy. The white box outlines the region shown in **d**. (**d**) Left, four para-aortic lymph nodes (LN) were identified (yellow arrows). Right, a sentinel node was positive for a light-emitting spot with GFP fluorescence expressed by HCT-116-GFP cells observed by fluorescence imaging (white arrowhead). Scale bar, 5 mm.

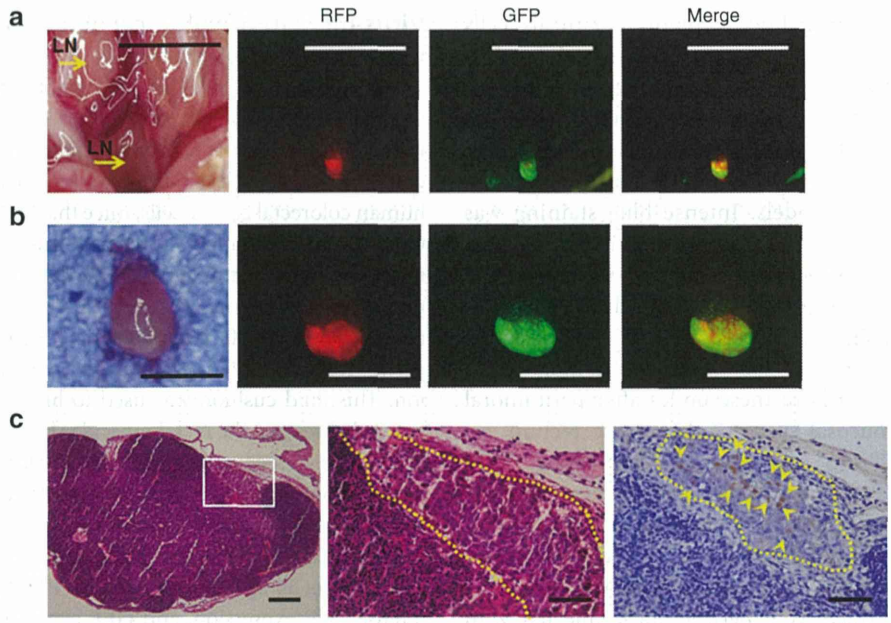

Figure 3 Lymphatic spread of the virus and selective replication in metastatic foci in regional lymph nodes. Mice bearing HCT-116-RFP primary rectal tumors that developed lymph node metastasis were peritumorally injected with 1×10^8 PFU of GFP-expressing OBP-401 into the submucosal space of the rectum. Virus spread and replication were assessed at laparotomy 6 days after virus administration. Three mice used for this study and analyses of a representative mouse are shown. (**a**) Gross localization of tumor-derived RFP and virus-induced GFP expression in the abdominal cavity of a representative mouse. The merged image shows that RFP-expressing metastatic foci in the sentinel lymph node were labeled with GFP fluorescence by OBP-401, indicating the successful delivery and replication of the virus in metastatic lymph nodes. Scale bars: 5 mm. (**b**) Excised metastatic lymph node of **a**. Scale bar: 2 mm. (**c**) Histopathological examination of excised metastatic lymph nodes. Left, hematoxylin and eosin staining showing metastatic foci. Scale bar, 200 μm; middle, detail of the boxed region of the left panel. Scale bar, 50 μm; right, immunohistochemical staining for adenoviral E1A protein in a serial section showing selective viral replication within tumor cells. The nuclei were counterstained with hematoxylin. Positive staining is reddish brown (yellow arrowheads). Scale bar, 50 μm.

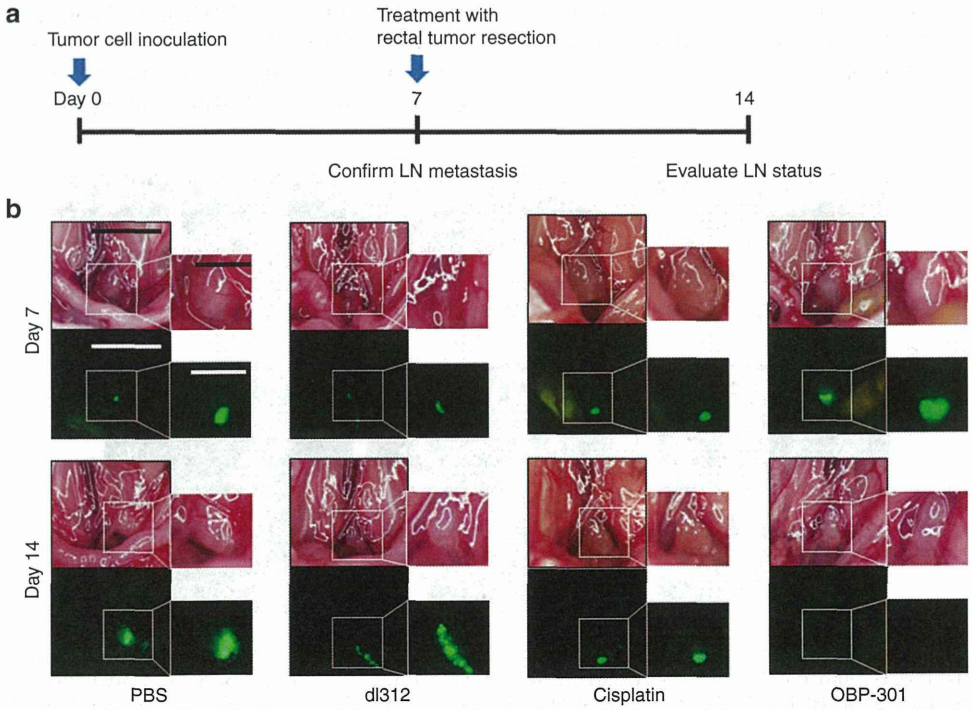

Figure 4 Biologically targeted ablation using OBP-301 eliminates metastatic foci on sentinel lymph nodes in an orthotopic colorectal cancer mouse model. (**a**) Treatment and evaluation schedule of animal experiments. (**b**) Macroscopic and fluorescence images of the abdominal cavity at laparotomy. Representative images among seven or eight mice with GFP-expressing metastatic foci in regional lymph nodes on day 7 of tumor inoculation are shown (top panels). Following treatment with mock (PBS), dl312, cisplatin, or OBP-301, the same mice were re-evaluated at laparotomy for the size and intensity of GFP signals on metastatic lymph nodes on day 14 (bottom panel). Scale bar, 5 mm (low magnification); 2 mm (high magnification).

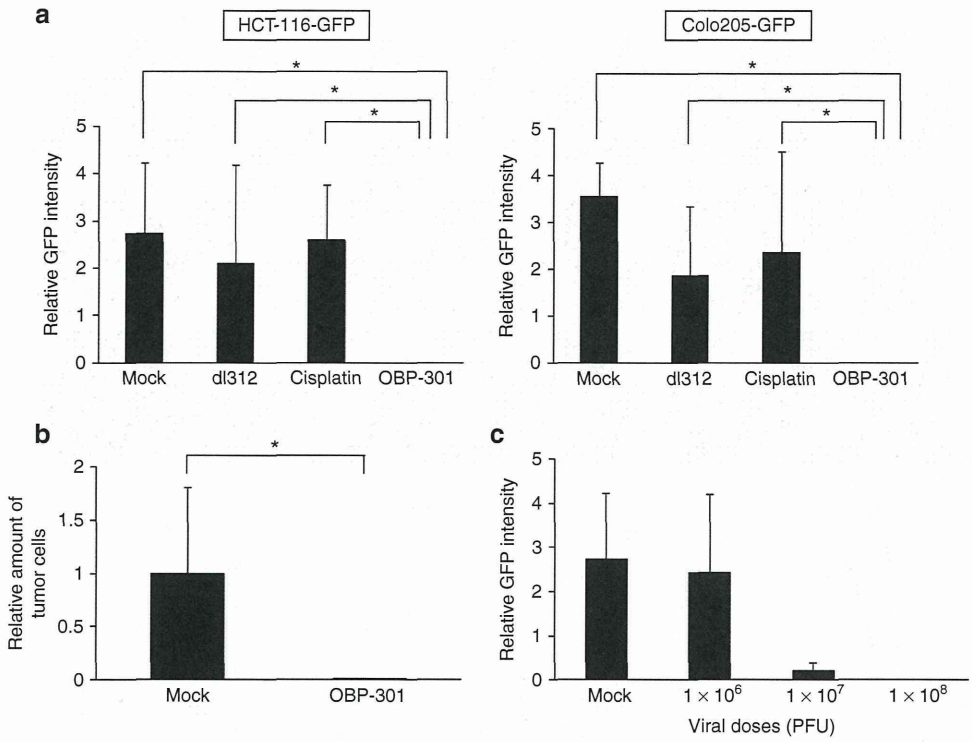

Figure 5 Quantitative analysis of the antitumor effect of OBP-301 on lymph node metastasis in an orthotopic colorectal cancer xenograft model. (**a**) The ratio of tumor cell-derived GFP intensity on metastatic lymph nodes of HCT-116-GFP (left panel) or Colo205-GFP (right panel) inoculated mice before and after the indicated treatments was calculated based on measurements of fluorescence images by using Image J software. We used seven or eight mice with Colo205-GFP cells and six mice with HCT116-GFP cells for each treatment group. Data are means ± SD. Statistical significance was defined as $P < 0.05$ (single asterisk). (**b**) Mice with established orthotopic early HCT-116-GFP tumors were treated with submucosal injection of 1×10^9 PFU of OBP-301 or dl312 followed by primary rectal tumor dissection on day 7 after tumor inoculation. Three mice were used for each group. Lymph nodes were harvested on day 14, and DNA was then extracted and subjected to quantitative *Alu* PCR analysis. The number of metastatic tumor cells is defined as the *Alu*/*GAPDH* ratio relative to that of the mock (PBS)-treated sample (mock = 1). Data are shown as means ± SD. Statistical significance was defined as $P < 0.05$ (single asterisk). (**c**) A dose-dependent purging effect of OBP-301 on metastatic lymph nodes. Mice with orthotopic early HCT-116-GFP tumors received a submucosal injection of OBP-301 at the indicated MOIs on day 7 and were subsequently subjected to GFP image-based quantification of lymph node metastasis on day 14. The numbers of mice used in this experiment are eight (mock) and four each (viral treatments). Data are shown as means ± SD.

PFU/30 μl PBS) failed to eliminate GFP fluorescence, indicating that these virus-mediated purging effects on metastatic lymph nodes were dose-dependent (**Figure 5c**).

Sustained metastatic tumor eradication by virus-mediated biological ablation

Finally, to assess if OBP-301-mediated biological ablation exerted prolonged antitumor effects, metastatic lymph nodes were visualized at laparotomy at 1 and 4 weeks after treatment using fluorescence imaging. In mice that received PBS or dl312, all metastatic lymph nodes grew larger in a time-dependent manner, although the magnitude of the enlargement varied between individual mice. Preinjection of cisplatin also did not affect tumor progression in the lymph nodes (**Supplementary Figure S6**). On the other hand, mice pretreated with OBP-301 showed no GFP fluorescence for at least 4 weeks after primary tumor resection (**Figure 6** and **Supplementary Figure S6**). Histopathological examination confirmed that virally purged lymph nodes were relapse-free (data not shown). These results suggest that submucosal preinjection of OBP-301 followed by primary tumor resection sustainably prevented metastatic tumor relapse over a long period.

DISCUSSION

The standard of care for treatment of intramucosal neoplastic lesions of the esophagus, stomach and colorectum is now a patient-friendly ESD that enables en-block resection of cancerous lesions regardless of size, since intramucosal tumors rarely metastasize to the lymph node.[2,23–25] However, when tumors penetrate slightly deeper into the submucosal layer, the incidence of nodal metastasis appears to increase significantly and, therefore, these patients are referred for complementary surgery with regional lymph node dissection.[10,11,26] Here, we describe a more effective and less invasive biological management for lymphatic metastasis that uses the telomerase-specific, replication-selective, oncolytic adenovirus OBP-301 and that employs submucosally invaded early rectal cancer orthotopic mouse models. In place of surgical lymphadenectomy we used a solution containing a tumor-killing virus as a submucosal cushioning agent before resection of the primary tumor. From a clinical viewpoint, this new, simple, and robust strategy is a more realistic and promising bench-to-bedside translation than prophylactic surgery for ablation of potential lymph node metastases in early gastrointestinal cancer patients.